

*Supplement of*

# **Chemical Characteristics and Source of PM<sub>2.5</sub> in Hohhot, a Semi-arid City in Northern China: Insight from the COVID-19 Lockdown**

Haijun Zhou<sup>1,2,3#</sup>, Tao Liu<sup>4#</sup>, Bing Sun<sup>5</sup>, Yongli Tian<sup>4</sup>, Xingjun Zhou<sup>4</sup>, Feng Hao<sup>4</sup>, Xi Chun<sup>1,2,3</sup>, Zhiqiang Wan<sup>1,2,3</sup>, Peng Liu<sup>1</sup>, Jingwen Wang<sup>1</sup>, Dagula Du<sup>6</sup>

<sup>1</sup>College of Geographical Sciences, Inner Mongolia Normal University, Hohhot 010022, China

<sup>2</sup>Provincial Key Laboratory of Mongolian Plateau's Climate System, Inner Mongolia Normal University, Hohhot 010022, China

<sup>3</sup>Inner Mongolia Repair Engineering Laboratory of Wetland Eco-environment System, Inner Mongolia Normal University, Hohhot 010022, China

<sup>4</sup>Environmental Monitoring Center Station of Inner Mongolia, Hohhot 010011, China

<sup>5</sup>Hohhot Environmental Monitoring Branch Station of Inner Mongolia, Hohhot 010030, China

<sup>6</sup>Environmental Supervision Technical Support Center of Inner Mongolia, Hohhot 010011, China

*Correspondence to:* \_Haijun Zhou (hjzhou@imnu.edu.cn)

**Table S1.** Summary of error estimation diagnostics from BS and DISP over the year

<b>BS Mapping</b>	CC	BB	CD	SIA	VE	CS	Unmapped
CC	100	0	0	0	0	0	0
BB	0	86	0	8	6	0	0
CD	0	0	100	0	0	0	0
SIA	0	0	0	100	0	0	0
VE	0	0	0	0	100	0	0
CS	0	0	0	4	0	96	0

<b>DISP</b>							
<b>Diagnostics</b>							
Error Code:	0						
Largest Decrease in Q:	-0.042						
%dQ:	-0.0003						
Swaps by Factor:	0	0	0	0	0	0	

CC, VE, CS, CD, SIA, and BB present coal combustion, vehicular emission, crustal source, construction dust, secondary inorganic aerosol, and biomass burning, respectively.

**Table S2.** Summary of error estimation diagnostics from BS and DISP in spring

<b>BS Mapping</b>	VE	CD	SIA	CS	CC	BB	Unmapped
VE	96	2	1	0	1	0	0
CD	2	98	0	0	0	0	0
SIA	0	0	100	0	0	0	0
CS	0	0	0	100	0	0	0
CC	0	0	0	0	100	0	0
BB	0	0	0	0	0	100	0

<b>DISP</b>							
<b>Diagnostics</b>							
Error Code:	0						
Largest Decrease in Q:	-0.0430						
%dQ:	-0.0017						
Swaps by Factor:	0	0	0	0	0	0	

**Table S3.** Summary of error estimation diagnostics from BS and DISP in summer

<b>BS Mapping</b>	SIA	Unknown	CS	BB	VE	CC	Unmapped
SIA	100	0	0	0	0	0	0
Unknown	0	98	0	0	2	0	0
CS	1	1	95	0	3	0	0
BB	1	0	0	87	10	1	1
VE	2	0	0	0	95	3	0
CC	5	0	0	0	1	94	0

<b>DISP</b>	
<b>Diagnostics</b>	
Error Code:	0
Largest Decrease in Q:	-0.1070
%dQ:	-0.0045
Swaps by Factor:	0

**Table S4.** Summary of error estimation diagnostics from BS and DISP in autumn

<b>BS Mapping</b>	CD	CC	SIA	BB	CS	VE	Unmapped
CD	100	0	0	0	0	0	0
CC	1	99	0	0	0	0	0
SIA	0	0	100	0	0	0	0
BB	2	1	3	90	2	1	1
CS	0	2	0	0	96	2	0
VE	0	0	0	0	0	100	0

<b>DISP</b>	
<b>Diagnostics</b>	
Error Code:	0
Largest Decrease in Q:	-0.3860
%dQ:	-0.0109
Swaps by Factor:	0

**Table S5.** Summary of error estimation diagnostics from BS and DISP in winter

<b>BS Mapping</b>	BB	SIA	CS	CC	CD	VE	Unmapped
BB	93	1	0	3	1	2	0
SIA	0	100	0	0	0	0	0
CS	0	0	100	0	0	0	0
CC	0	0	0	100	0	0	0
CD	0	0	0	3	90	7	0
VE	0	0	0	0	0	100	0
<b>DISP</b>							
<b>Diagnostics</b>							
Error Code:	0						
Largest Decrease in Q:	-0.0400						
%dQ:	-0.0017						
Swaps by Factor:	0	0	0	0	0	0	

**Table S6.** Comparison of chemical composition of PM<sub>2.5</sub> in Hohhot and other cities.

Location	Date type	period	PM <sub>2.5</sub> ( $\mu\text{g}/\text{m}^3$ )	Percentage (%)								Reference	
				OM	SO <sub>4</sub> <sup>2-</sup>	NO <sub>3</sub> <sup>-</sup>	NH <sub>4</sub> <sup>+</sup>	Cl <sup>-</sup>	EC	MD	others		
Hohhot	Offline	pre-LD	108.7	27.8	24.4	22.9	8.0	2.9	4.6	4.7	4.7	This study	
		LD	68.3	30.5	17.2	18.0	4.9	3.9	5.4	11.8	8.2		
		post-LD	32.6	35.0	9.5	10.2	1.8	2.8	7.5	18.9	14.2		
		annual	42.6	31.5	13.4	12.3	3.3	2.5	6.6	14.2	16.1		
Xi'an	online	pre-LD	102.0	42	7	30	13	3	-	-	8	(Tian et al., 2021)	
		LD	60.2	48	8	25	12	3	-	-	7		
Tianjin	online	Same period in 2019	LD	-	10.6	9.8	20.2	9.7	2.8	3.1	-	43.8	(Ding et al., 2021)
				-	13.7	8.3	14.5	8.2	4.0	3.6	-	47.7	
Guangzhou	online	pre-LD	-	18.2 <sup>a</sup>	19.5	37.8	21.4	-	3.1	-	-	(Wang et al., 2021)	
		LD	-	35.2 <sup>a</sup>	20.3	18.7	22.1	-	3.8	-	-		
Beijing	online	pre-LD	32.2	18.3	12.1	22.2	14.2	3.6	3.0	-	26.5 <sup>c</sup>		
		LD	50.0	15.8	16.1	26.1	16.1	3.0	2.6	-	20.4 <sup>c</sup>		
Nanjing	online	pre-LD	68.2	12.3	18.0	34.4	15.8	1.9	2.5	-	15.3 <sup>c</sup>	(Ren et al., 2021)	
		LD	44.0	17.9	21.5	24.7	14.1	3.2	1.9	-	16.8 <sup>c</sup>		
Changsha	online	pre-LD	59.6	16.8	11.3	26.7	12.7	1.2	2.2	-	29.0 <sup>c</sup>		
		LD	36.6	20.8	12.5	14.2	9.2	1.5	1.3	-	40.5 <sup>c</sup>		
Shanghai	online	pre-LD	60.9	23.5 <sup>b</sup>	18.6	37.5	19.3	1.2	-	-	-	(Chen et al., 2020)	
		LD	41.2	39.5 <sup>b</sup>	21.0	29.4	18.4	1.7	-	-	-		
		post-LD	34.0	25.5 <sup>b</sup>	27.4	26.6	19.1	1.5	-	-	-		

<sup>a</sup> The sum of POC and SOC. <sup>b</sup> Sum of oxygenated and hydrocarbon-like organic aerosols. <sup>c</sup> Sum of trace elements and unidentified. “-” present no data available in the reference. Pre-LD, LD, and post-LD present pre-lockdown, lockdown, and post-lockdown period, respectively.

**Table S7.** Comparison of source contribution of PM<sub>2.5</sub> in Hohhot during pre-LD, LD, post-LD, and over the year.

Location	Date type	Model	PM <sub>2.5</sub> (μg/m <sup>3</sup> )	Source contribution (%)								Reference
				period	CC	VE	DS	SIA	BB	SS	IP	
Hohhot	Offline	PMF	32.4	Spring	56.1	17.0	22.6 <sup>a</sup>	4.2	-	-	-	This study
			24.3	Summer	24.0	48.4	19.7 <sup>a</sup>	5.3	2.6	-	-	
			37.0	autumn	38.9	33.8	16.1 <sup>a</sup>	11.1	-	-	-	
			80.8	winter	65.4	14.3	6.8 <sup>a</sup>	10.5	-	-	-	
			42.6	annual	38.3	35.0	13.5 <sup>a</sup>	11.4	1.7	-	-	
Tianjin	Offline	PMF	60.1	annual	25	21	7	30	-	2 <sup>b</sup>	5	(Tian et al., 2021)
	Online	PMF	54.3	annual	24	18	4	38	-	1 <sup>b</sup>	4	
Shanghai	Offline	PMF	73.7	annual	2.4	18.3	4.6	31.6	12.3	10.6 <sup>c</sup>	20.2	(Feng et al., 2022)
Beijing	Offline	PMF	-	annual	11.1	24.7	4.3	48.1 <sup>d</sup>	11.7	-	-	(Zkov áet al., 2016)

CC, VE, DS, SIA, BB, SS, IP present coal combustion, vehicular emission, dust source, secondary inorganic aerosol, biomass burning, sea salt, and industrial process, respectively. “-” present no data available in the reference. <sup>a</sup> Sum of CS and CD contributions in this study. <sup>b</sup> Sum of SS and BB. <sup>c</sup> Ship emission. <sup>d</sup> Sum of secondary sulfate and secondary nitrate. Pre-LD, LD, and post-LD present pre-lockdown, lockdown, and post-lockdown period, respectively.

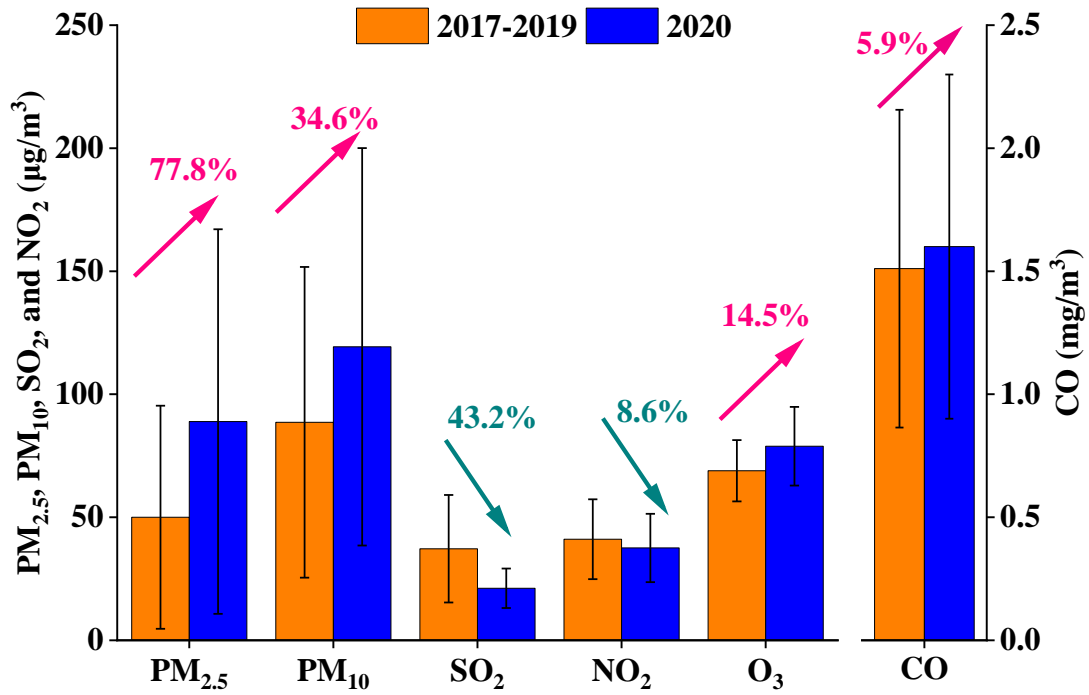


**Figure S1.** Comparison of air pollutants in Hohhot during the LD period with the same period in 2017-2019.

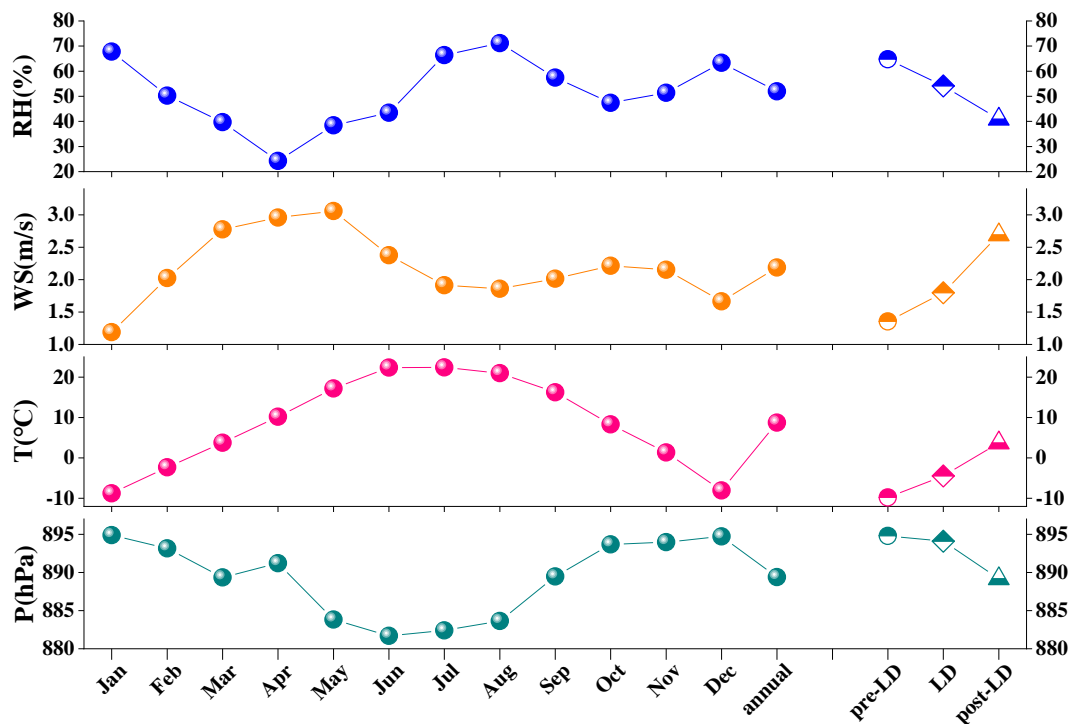


**Figure S2.** Monthly variation of (a) RH, (b) WS, (c) T, and (d) P in Hohhot during the sampling period.

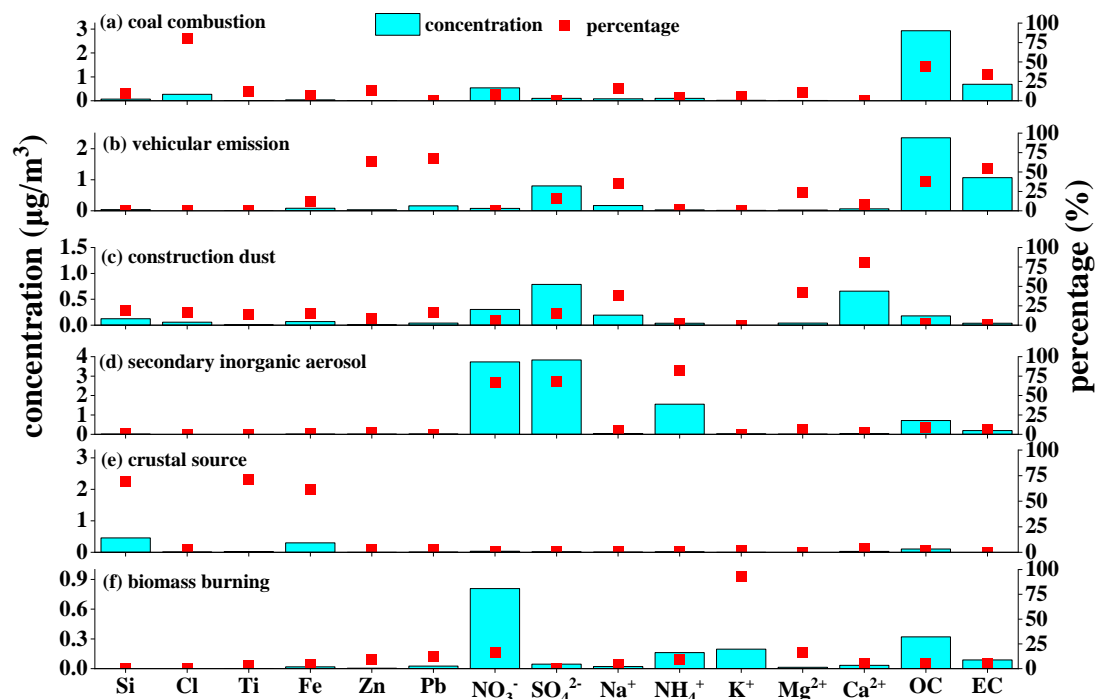


Figure S3. Source profiles of PMF for annual.

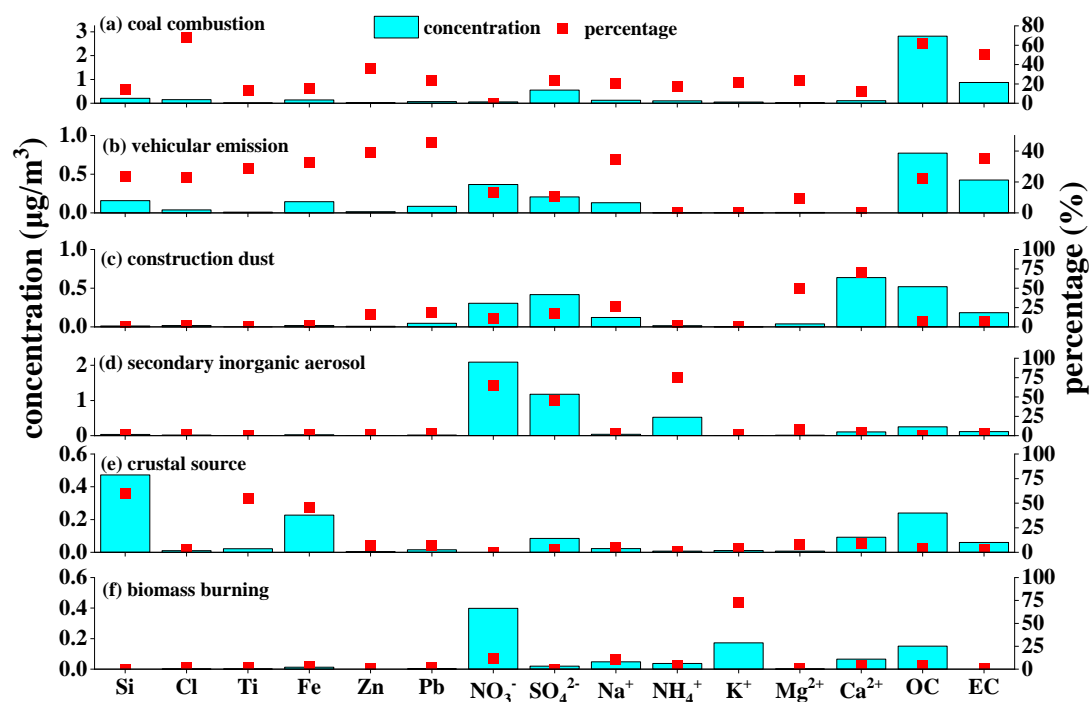


Figure S4. Source profiles of PMF for spring.

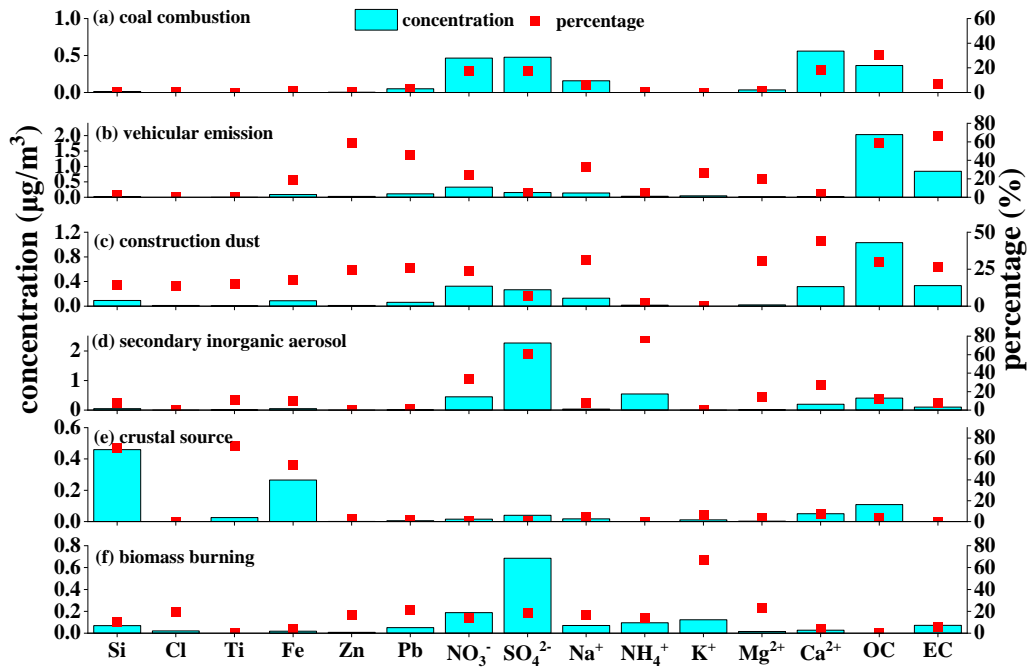


Figure S5. Source profiles of PMF for summer.

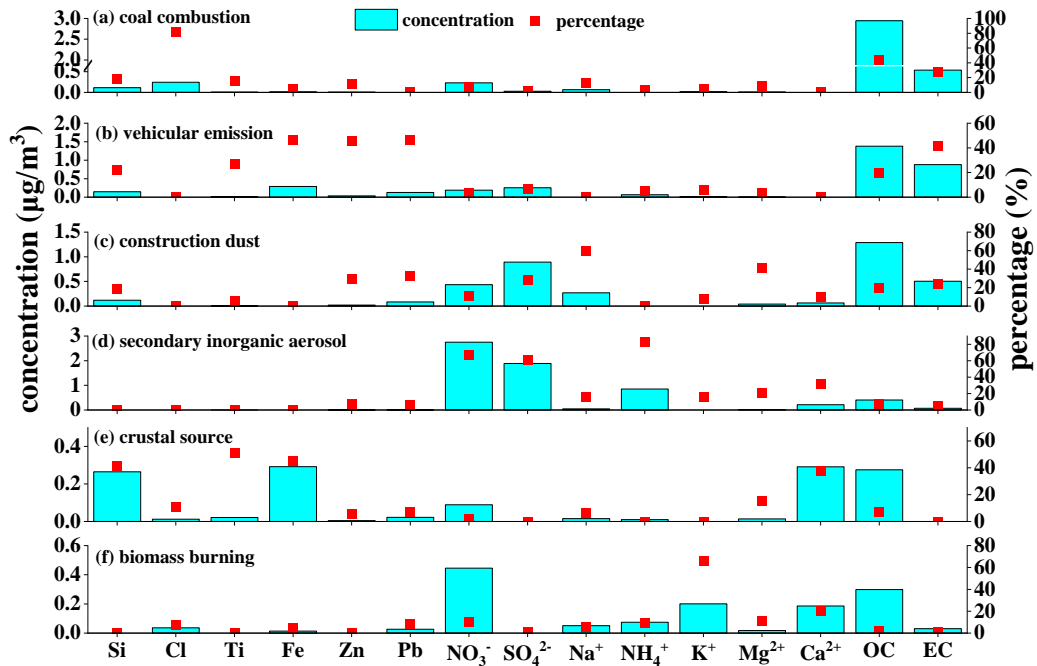
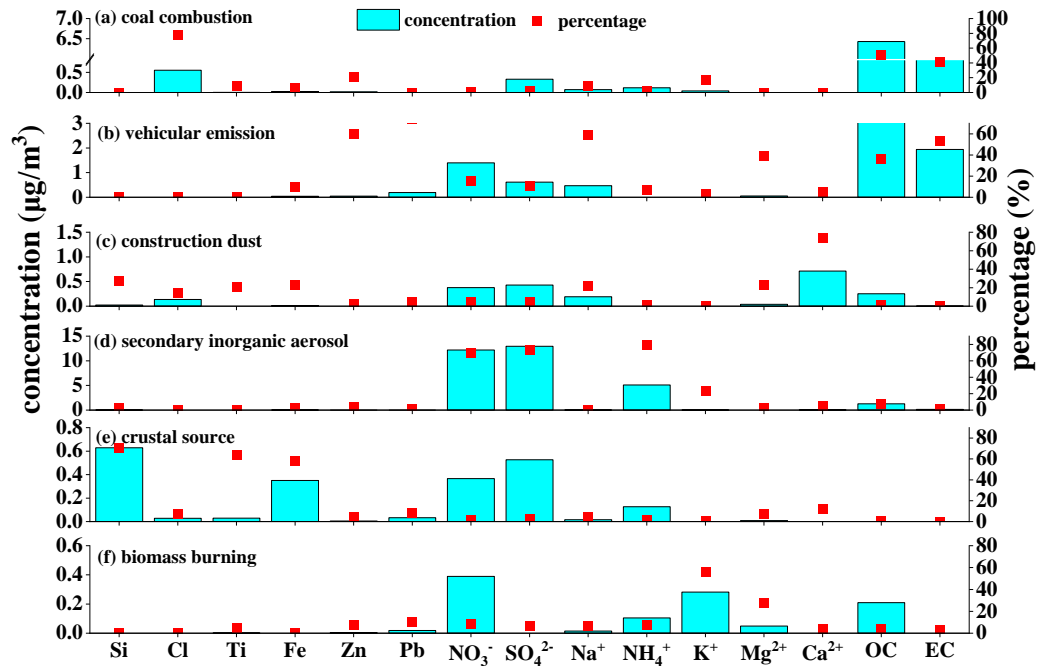


Figure S6. Source profiles of PMF for autumn.



**Figure S7.** Source profiles of PMF for winter.

## References:

- Chen, H., Huo, J., Fu, Q., Duan, Y., Xiao, H., and Chen, J., 2020. Impact of quarantine measures on chemical compositions of PM<sub>2.5</sub> during the COVID-19 epidemic in Shanghai, China, *Science of The Total Environment*, 743, 140758, <https://doi.org/10.1016/j.scitotenv.2020.140758>.
- Ding, J., Dai, Q., Li, Y., Han, S., Zhang, Y., and Feng, Y., 2021. Impact of meteorological condition changes on air quality and particulate chemical composition during the COVID-19 lockdown, *Journal of Environmental Sciences*, 109, 45-56, <https://doi.org/10.1016/j.jes.2021.02.022>.
- Feng, X., Feng, Y., Chen, Y., Cai, J., Li, Q., and Chen, J., 2022. Source apportionment of PM<sub>2.5</sub> during haze episodes in Shanghai by the PMF model with PAHs, *Journal of Cleaner Production*, 330, 129850, <https://doi.org/10.1016/j.jclepro.2021.129850>.
- Ren, C., Huang, X., Wang, Z., Sun, P., Chi, X., Ma, Y., Zhou, D., Huang, J., Xie, Y., Gao, J., and Ding, A., 2021. Nonlinear response of nitrate to NO<sub>x</sub> reduction in China during the COVID-19 pandemic, *Atmospheric Environment*, 264, 118715, <https://doi.org/10.1016/j.atmosenv.2021.118715>.
- Tian, J., Wang, Q., Zhang, Y., Yan, M., Liu, H., Zhang, N., Ran, W., and Cao, J., 2021. Impacts of primary emissions and secondary aerosol formation on air pollution in an urban area of China during the COVID-19 lockdown, *Environment International*, 150, 106426, <https://doi.org/10.1016/j.envint.2021.106426>.
- Wang, N., Xu, J., Pei, C., Tang, R., Zhou, D., Chen, Y., Li, M., Deng, X., Deng, T., Huang, X., and Ding, A., 2021. Air quality during COVID-19 lockdown in the Yangtze River Delta and the Pearl River Delta: Two different responsive mechanisms to emission reductions in China, *Environmental Science & Technology*, 55, 5721-5730, <https://doi.org/10.1021/acs.est.0c08383>.
- Zková N., Wang, Y., Yang, F., Li, X., Tian, M., and Hopke, P. K., 2016. On the source contribution to Beijing PM<sub>2.5</sub> concentrations, *Atmospheric Environment*, 134, 84-95, <https://doi.org/10.1016/j.atmosenv.2016.03.047>.